

FORMATION PARAMETERS OF THE LOWER EOCENE ROCKS IN QATAR

A. A. EL-SAYED*

Department of Geology, University of Qatar

Key words : Porosity, Permeability, Rus Formation, Qatar.

ABSTRACT

The study of some carbonate rock samples collected from four different locations in Qatar and attributed to the Rus Formation (Lower Eocene) reveals that these rocks are mainly heterogeneous in their petrophysical characteristics. This was indicated not only by study of pore space geometry but also by a skewed distribution of porosity, permeability, and hydraulic conductivity measured data.

Parameters enhance reservoir evaluation and description were estimated. Whereas, useful empirical relations have been derived by which both the storage capacity and the gas—permeability of the studied rocks can be determined. Study of SEM—micrographs has shown the influence of post—depositional processes on both porosity and gas—permeability with different degrees of performance.

INTRODUCTION

Qatar Peninsula is an arid region covering about 11437 sq.km and protruding into the Arabian Gulf as an eastern appendix to the Arabian Peninsula (Fig. 1). It lies between latitudes $24^{\circ}30'$ and $26^{\circ}10'$. The landscape of Qatar is generally flat and low lying except for some modest hills to the north west. The exposed stratigraphic succession in Qatar is composed mainly of Tertiary limestones and dolomites with interbedded clays, shales, and marls covered locally with Quaternary and Recent deposits (Fig. 2). The oldest exposed rocks in Qatar are the Lower Eocene limestones of the Rus Formation. The greater part of the land surface consists of dolomites and limestones. Comprehensive studies have been dealt with the sedimentology, primary structures, and stratigraphy of the Eocene rocks in Qatar (Cavelier, 1970; Purser, 1973; Abu-Zeid and Khalifa, 1983; Abu-Zeid and Boukhary, 1984; Hamam, 1984; and Boukhary, 1985).

* *Permanent address* : Department of Geology, Faculty of Science, Ain Shams Univ., Cairo, Egypt.

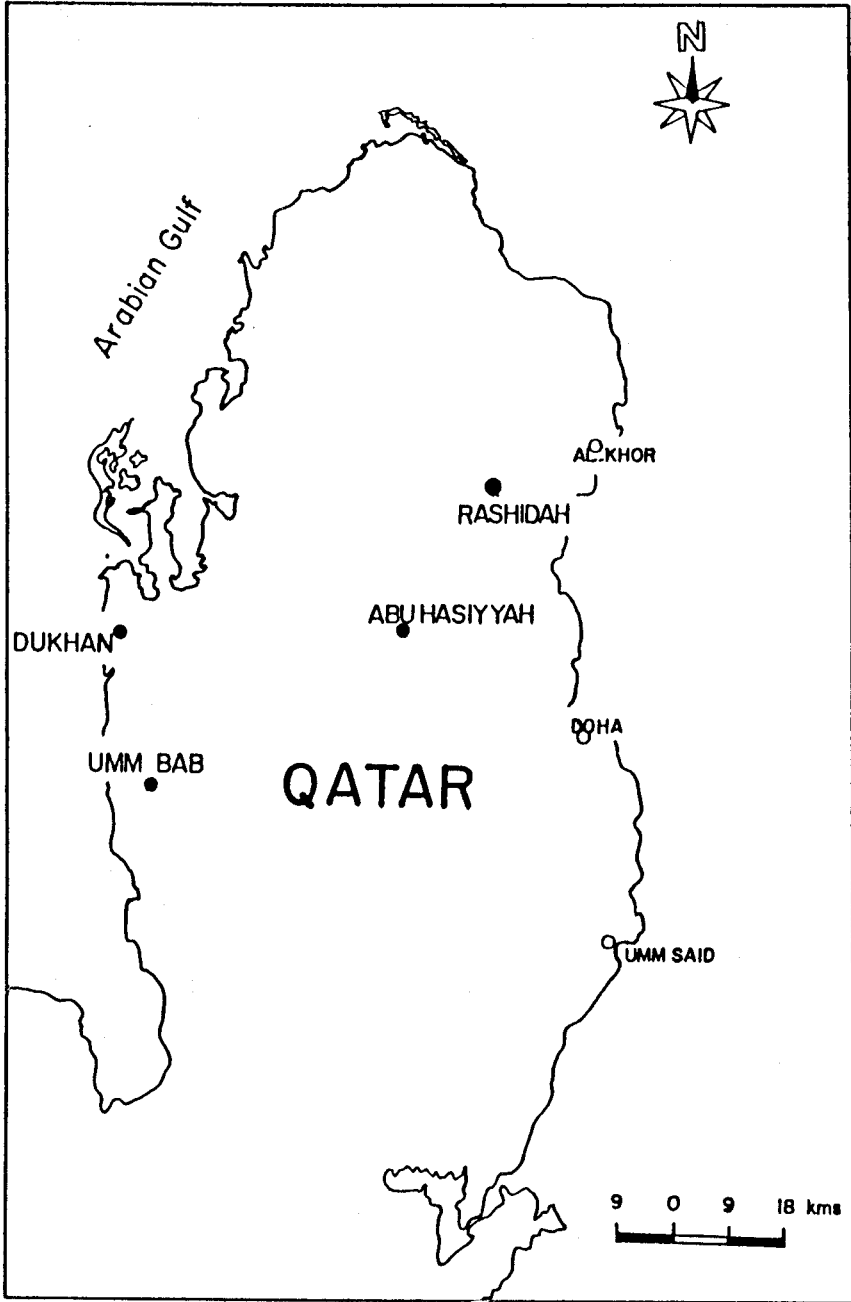


Fig.1. Location map of the study areas.

AGE				LITHOSTRATIGRAPHIC UNITS.	
				GROUP	FORMATION
CENOZOIC	QUATERNARY.				SUPERFICIAL DEPOSITS
	TERTIARY.	MIO - PLOCENE			HOFUF
					DAM
		LUTETIAN	ARUMA	DAMMAM	
		YPRESIAN		RUS	
		THANETIAN MOHTIAN?		UMM ER RADHUMA	
	MESOZOIC	CRETACEOUS	UPPER	MAASTRICHTIAN	SIMSIMA
CAMPANIAN				FIGA	
SANTONIAN				HALUL	
CONIACIAN				LAFFAN	

Fig. 2. Stratigraphic Setting of Rus Formation (After Hamam, 1984).

The rock samples used in the present study are representing only the upper part of the Rus Formation. They are obtained from four different areas (black circles in Fig. 1). The Rus Formation is overlain, apparently conformably, by the Dammam Formation. It is considered as one of the main effective aquifers in both Qatar and many of the Arabian Gulf states. An accurate reservoir rock description is essential for effective management of water producing formations. The areal variation of aquifer parameters such as porosity, permeability, hydraulic conductivity, and effective thickness influences both water recovery and distribution. This paper is an attempt to establish comprehensive interrelationships which may enable one to determine the most significant factors influencing both the flow and the storage capacity properties of the Rus Formation.

METHODS AND TECHNIQUES

Laboratory measurements of both rock porosity and gas-permeability for 13 limestone core samples (Table-1) followed methods adopted by Anderson (1975). Gas-permeability measurements were conducted with Hassler-type core holder in which samples (approximately 0.025 m in diameter and 0.05 m long) were subjected to dry Nitrogen gas with pressure of 1378.9514 kpa. The permeability (k) is calculated as;

$$k \text{ (in } \mu\text{m}^2 \text{)} = \frac{C \cdot Q \cdot hw \cdot L^2}{200 \times V_b} \times 9.869 \times 10^{-4} \quad (1)$$

Where : C = value of mercury height, mm.

Q = orifice value.

hw = orifice manometer reading, mm.

L = sample length, cm.

V_b = sample bulk volume, cubic cm.

Porosity data were determined by use of both the mercury pump universal porosimeter for bulk volume (V_b) determination and the Helium porosimeter with matrix cup core holder for grain volume (V_g) estimation. Hence, porosity is calculated as;

Table 1
Laboratory Measured Parameters For Samples Obtained From The Rus Formation.

Sample Number	Pilot Area	C.Q.hw (mm)	V _b cm ³	L ² cm ²	V _p cm ³	Ø, %	k, μm ²	K, × 10 ⁻⁸ m / s
R - 1 A	Abu-Hasiyyah	074977.43	20.775	17.556	4.293	20.66	0.3226	329.00
R - 2 A	Abu-Hasiyyah	110238.31	17.100	12.250	3.350	19.59	0.3897	411.00
R - 3 U	Umm-Bab	103178.94	23.580	22.944	2.937	12.45	0.4954	522.00
R - 4 U	Umm-Bab	003450.42	20.540	17.556	3.038	14.79	0.0146	015.00
R - 5 D	Dukhan	004299.25	17.530	15.840	3.100	17.68	0.0192	020.00
R - 6 D	Dukhan	067533.63	14.940	09.859	5.480	36.68	0.2199	232.00
R - 7 D	Dukhan	046495.24	17.335	12.180	6.015	34.70	0.1346	142.00
R - 8 D	Dukhan	001796.79	16.830	11.560	3.540	21.03	0.61 × 10 ⁻⁴	006.00
A - 7 U	Umm-Bab	078753.27	13.670	07.562	1.304	09.53	0.2149	227.00
A - 1 A	Abu-Hasiyyah	000088.95	14.930	08.702	1.310	08.77	0.26 × 10 ⁻³	000.26
Ra 7 R	Rashidah	005947.34	17.930	12.496	3.549	19.79	0.0204	022.00
Ra 7 R	Rashidah	016094.36	17.570	12.250	2.809	15.99	0.0554	058.00
Ra 9 R	Rashidah	009039.45	13.960	07.562	3.053	21.87	0.0241	025.00

$$\varnothing = 1.0 - \frac{V_g}{V_b} \quad 100 \quad (2)$$

Where \varnothing = porosity, per cent.

Out of the studied samples, only 4 samples were selected for scanning electron microscope examination (JEOL - 35). Microscope general description, principles, operations, and applications were discussed by Hashimoto and Suganuma (1973). Sample preparation and examination followed techniques adopted by Smith (1961) and Nicholas and Krinsley (1971).

POROSITY

The statistical analysis of the measured porosity data indicates that sample porosity is varied in a wide range. It varied from 8.77 to 36.68 %, with a mean porosity value equals 18.96 %. The calculated standard deviation of porosity data seems to be high ($\sigma_{\varnothing} = 8.02\%$). It may be confirm the skewed porosity distribution shown in Fig. 3A. The storage capacity of the studied samples was calculated and plotted (Fig. 3B) against porosity range. Figure 3B reveals that 98 % of the Rus Formation storage capacity are represented by samples having porosities of 12.0 % or greater. On the other hand, 30 % of the storage capacity are represented by samples having porosity $\leq 31.0\%$

GAS-PERMEABILITY

Gas permeability measurements (Tab. 1) of the studied samples were found to be varied from 2.56×10^{-4} to $0.495 \mu\text{m}^2$, with an average permeability value equals $0.1865 \mu\text{m}^2$. The calculated permeability standard deviation (σ_k) was found to be equal $0.8857 \mu\text{m}^2$. Its high value implies that we have more than one sample population being treated as single one (Fig. 4, dotted-line histogram).

The hydraulic conductivity (K) of a rock is known as the coefficient of permeability (k) of that rock. It is experimentally measured by Darcy (1856), while he deduced the following equation;

$$Q = -K \frac{\Delta h}{\Delta L} \cdot A \quad (3)$$

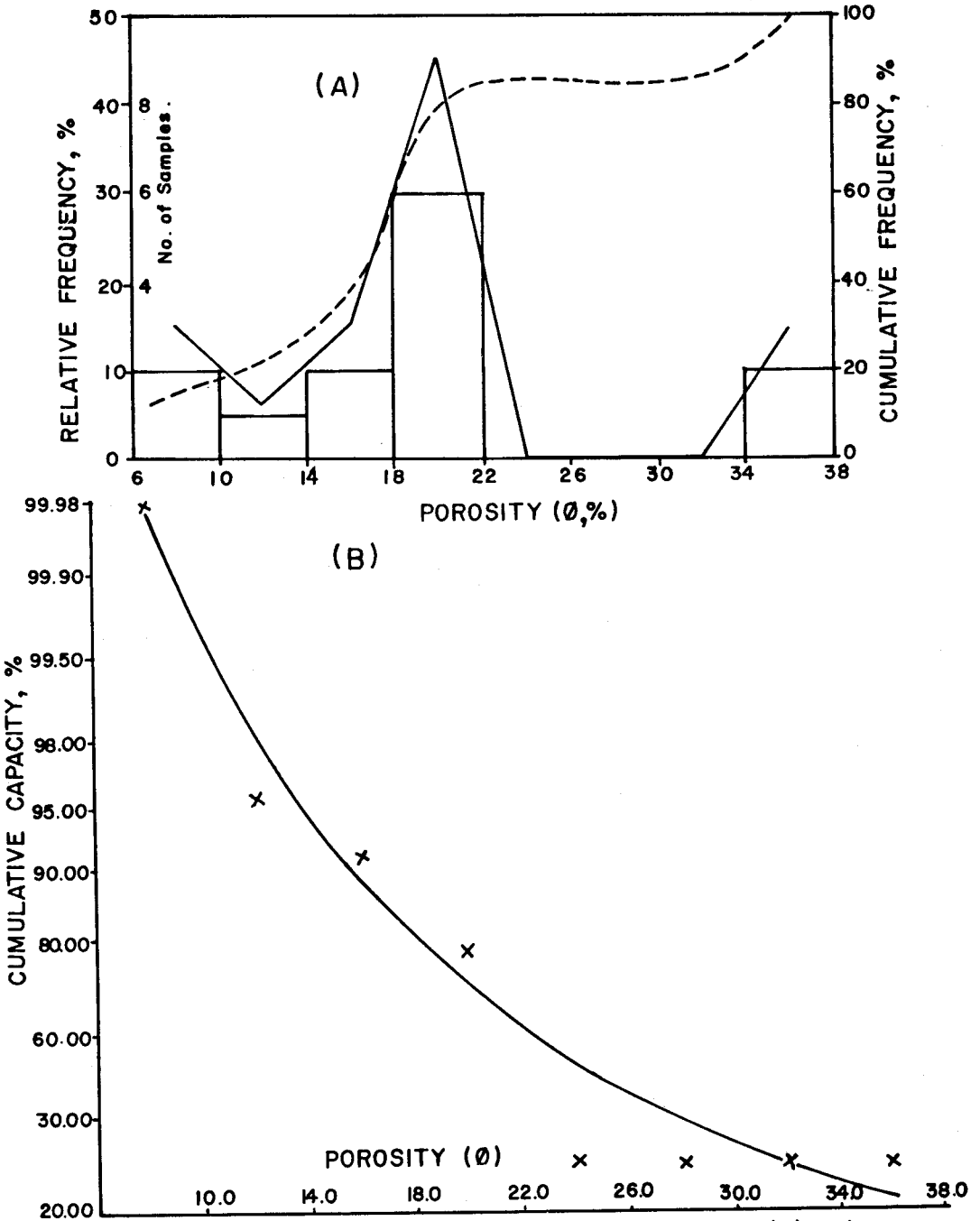


Fig (3). Porosity polygons and frequency distribution Curves (A) and porosity capacity (B)

Where : Q = volumetric rate of flow.,
($\Delta h / \Delta L$) = hydraulic gradient.
 A = cross - sectional area.

Therefore, hydraulic conductivity is a function not only of the porous medium but also of the fluid, while permeability is a function only of the medium itself (Davis, 1969). The calculated hydraulic conductivity (Tab. 1) was found to be varied from 2.6×10^{-9} to 522.0×10^{-8} m/s, with an average value equal 0.16×10^{-5} m/s (see Fig. 4; solid-line histogram). The calculated standard deviation ($\sigma_K = 0.912$ m/s) constitutes a fair inference for the heterogenesis of both rock pore space and pore throat-size distribution.

Figure 5, exhibits both the gas-permeability and the hydraulic conductivity capacity. This cross-plot shows that 98 % of both permeability and hydraulic conductivity capacity are represented by rock samples having permeability equal $2.6 \times 10^{-2} \mu\text{m}^2$ and hydraulic conductivity = 5.72×10^{-7} m/s or greater respectively. While 30 % of their capacity is represented by rock samples having permeability $\leq 6.3 \times 10^{-1} \mu\text{m}^2$ and hydraulic conductivity $\leq 6.99 \times 10^{-6}$ m/s respectively.

PORE VOLUME VS. LOG (k/ϕ) RATIO

An attempt was made to relate the volume of the sample pore space (V_p) to the logarithm of its permeability per porosity ratio ($\log k/\phi$). An examination of this relation (Fig. 6) reveals two linear trends (A & B). Each of them is represented by a reliable regression equation of high coefficient of correlation. The obtained trends (Fig. 6) are significantly discriminated by an average porosity value characterizing each of them. The calculated regression equations would be expected to give a plausible prediction of permeability of the Rus Formation when the porosity values are already known. The results show that the pore space volume for samples adopted trend (A) is equal to 1.36 times the pore space volume for that belonging to the trend (B), when (k/ϕ) ratio equals unity.

PERMEABILITY VS. POROSITY

Figure 7, shows the gas-permeability versus porosity relation, Although there was a considerable scattering in the data points, two different trends can be

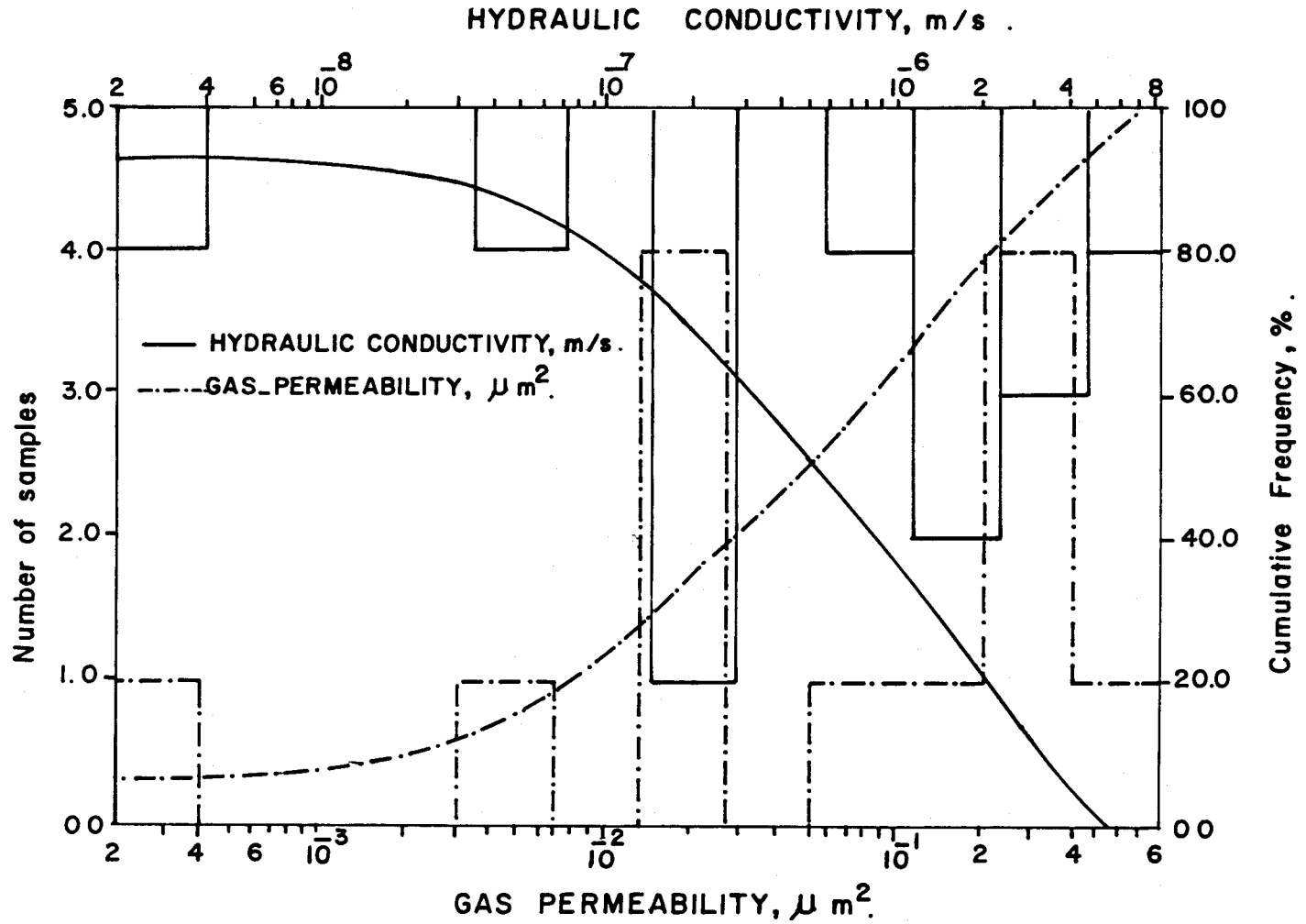
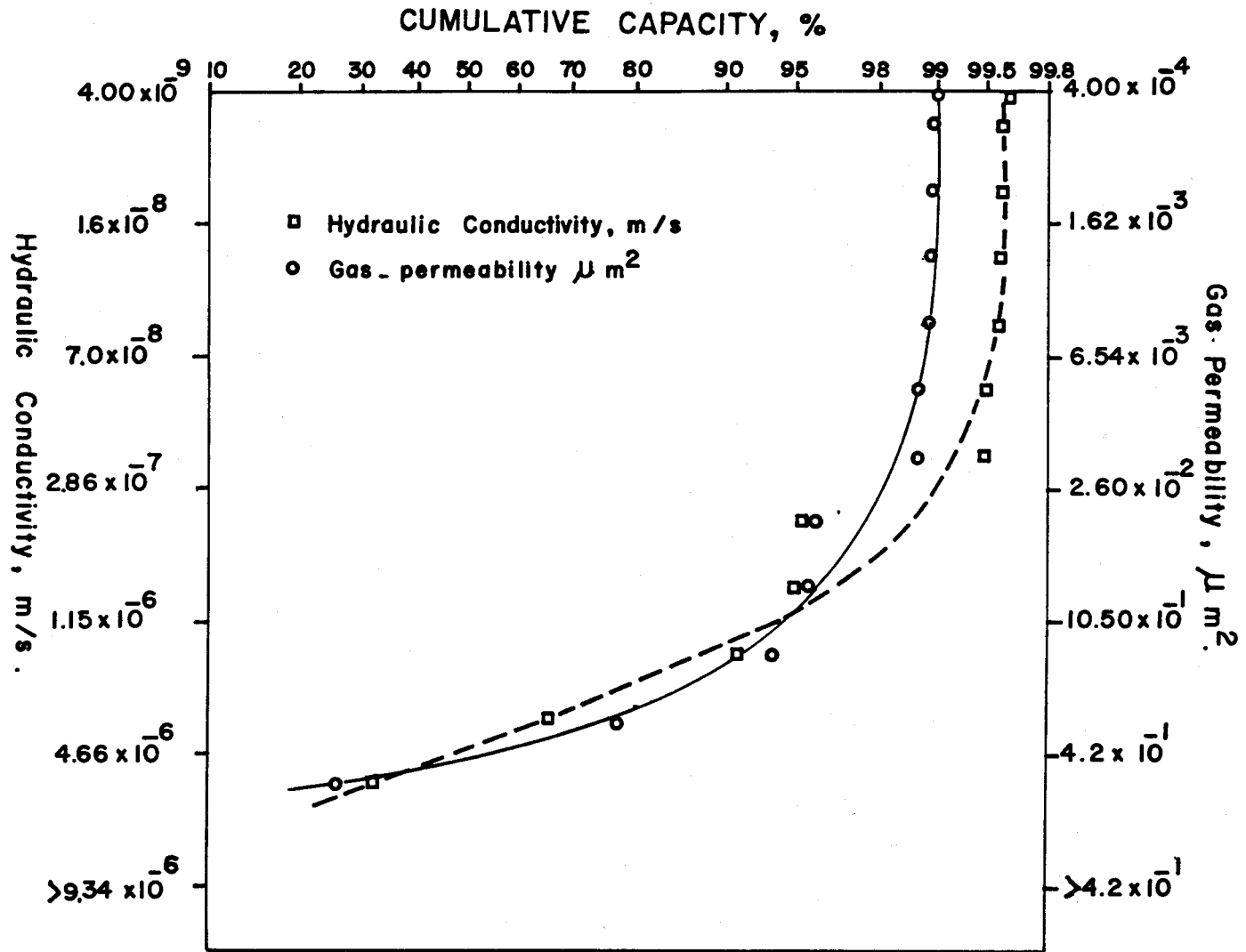


Fig.(4) Frequency polygone and cumulative frequency Distribution for both Gas_permeability and Hydraulic conductivity .



Fig(5) Gas Permeability and Hydraulic Conductivity Capacity.

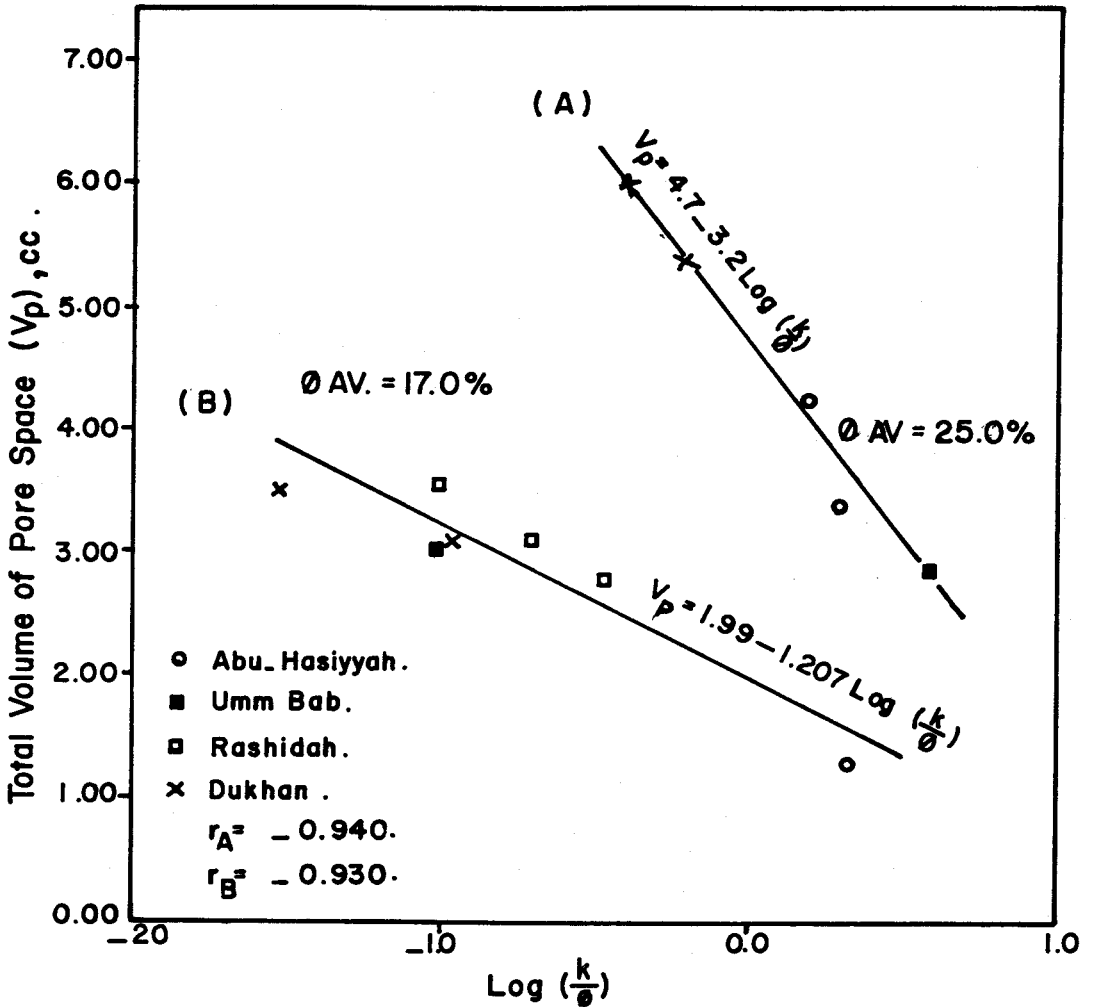


Fig.(6) Total volume of pore space versus Log (K/φ).

distinguished (A & B). The scattering of the data points may suggest differences in the nature of the pore networks. Hence the pore geometry is a resultant of several different diagenetic, that is, postdepositional, physical and chemical processes (Hearn *et al.*, 1984). Then, 4 samples were selected for studying their pore space geometry and its relations to both the rock-porosity and permeability by use of the scanning electron microscope. These samples are marked on Fig. 7. Two of them almost have an equal permeability, and differ in porosity, while the rest are almost have the same porosity and differ in permeability.

Figs. 8 a & b, reveal two SEM micrographs for rock samples (A-7U and R-6D) approximately having equal permeability and different porosity ($\phi = 9.539$ and 36.684% respectively). Clearly that sample A-7U is intraclastic limestone, poorly to intermediate sorted, and may be of shelf area, deep water sedimentation. Little amount of smectite is scattered across the rock pore throats. This may be due to hydrothermal mineral reactions of kaolinite and dolomite (Hutcheon and Oldershaw, 1985). The SEM micrograph (Fig. 8 a) exhibits large pores and pore throats of 25μ in size. Such pores constituted the most effective elements for increasing permeability. Low porosity could be explained by the observed blind pores (Fig. 8 a). The sample R-6D is mainly intraclastic clean washed limestone, moderately to well sorted, open pore spaces, characteristic for shallow water, strong currents and wave affected environment (Fig. 8 b). The SEM micrograph reveals a lot of dead ending capillary pores of 0.75μ in size. They are distributed over grain surfaces. This phenomenon can partly explain the obtained high porosity value of sample R-6D. Whereas meteoric water penetration may be able to create significant volumes of secondary porosity in the shallow subsurface (Giles and Marshall, 1986).

Figs. 8 c & d, show two SEM micrographs for rock samples (R-8D and R-1A) almost having equal porosity and different permeability ($k = 6.11 \times 10^{-3}$ and $0.31266\mu\text{m}^2$ respectively). The sample R-8D is partially dolomitic, poorly sorted, small dolomite rhombs are scattered through the rock pore spaces and across the pore throats. The SEM micrograph (Fig. 8 c) reveals a lot of dead ending pores and dolomite pore lining which can increase porosity at the expense of the permeability (El-Sayed, 1981). On the other hand, the micrograph (Fig. 8 d) exhibits a dolomitic limestone sample (R-1A). The intergrowth of dolomite crystals shows good rhombic shapes. It may be of supratidal flat, humid

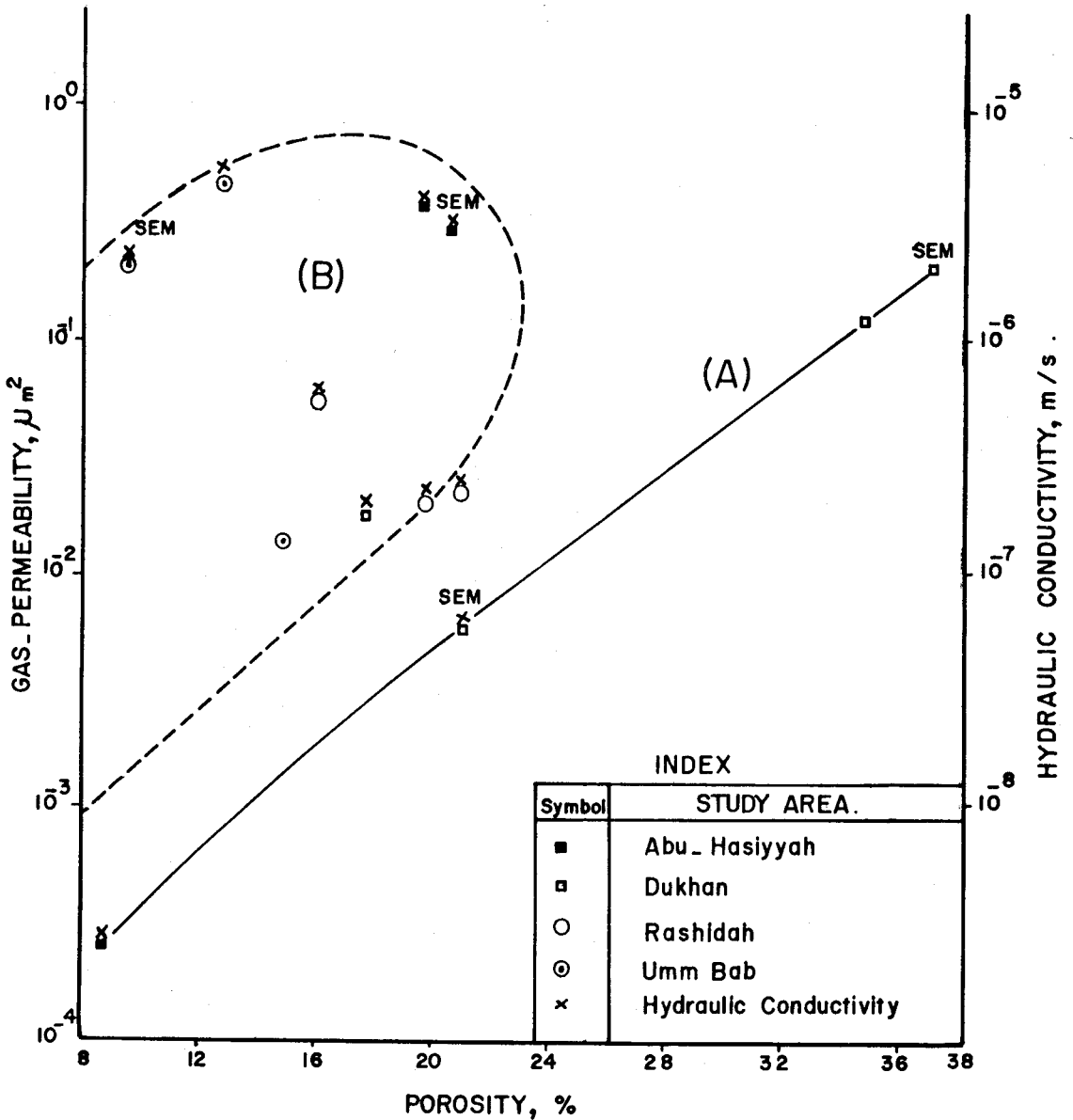


Fig.(7) POROSITY, PERMEABILITY AND HYDRAULIC CONDUCTIVITY RELATIONS.

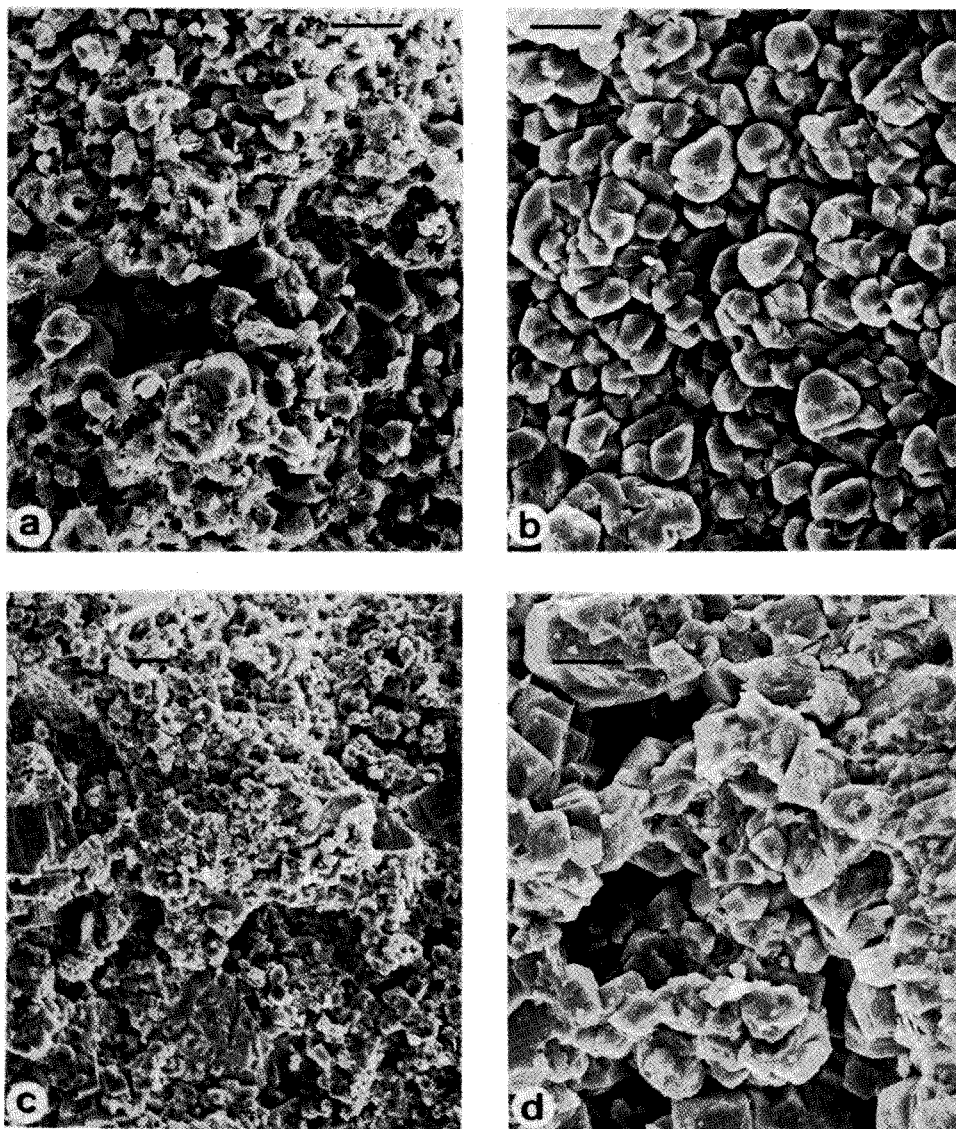


Fig. 8: Scanning electron micrographs of some limestone samples of the Rus Formation. a. General view of pore lined with semectite. The clay encrusts the rounded surface of detrital grains. b. General view shows many of dead ending capillary pores. c. Occluded pores with both small dolomite rhombs and calcite as pore fill. d. Large interconnected pores and pore throats. Scale for all micrographs $10\mu\text{m}$.

environment of sedimentation. It shows large uniform pores (20 – 30 μ in size) and pore throats. Desolution by meteoric water penetration and mixing corrosion (Giles and Marschall, 1986) are the possible porosity mechanism. It is concentrated near fractures and around large dolomite rhombs. Its high porosity value can be explained by the existence of large open pore spaces. While, the large (2 – 3 μ in size) open pore throats are mainly responsible for increasing permeability. It is worthy of mention that such rocks are classified as very good aquifers (Levorsen, 1967).

CONCLUSIONS

1. The measured rock porosity and permeability data are varied in a very wide range.
2. Reliable regression line equations have been obtained relating the rock pore volume (V_p) to the permeability per rock porosity (k/ϕ) ratio.
3. The porosity – permeability relation has been affected by smectite pore filling and dolomite pore lining side by side with desolution of some mineral grains.

ACKNOWLEDGEMENT

I am thankful to Mr. A. Galhoom for providing facilities during collection of the samples. Also, I am grateful to the Educational Technology Department of Qatar University for drafting the figures.

REFERENCES

- Abu-Zeid, M. M. and M. A. Boukhary 1984.** Stratigraphy, facies and environment of sedimentation of the Eocene rocks in the Fhailil (Gebel Dukhan) section, Qatar, Arabian Gulf, *Revue de Paléobiologie* 3 : 159 – 173.
- Abu-Zeid, M. M. and H. Khalifa 1983.** Sedimentological and paleoenvironmental aspects of the Miocene succession in Gebel Al-Nikhsh, Qatar, Arabian Gulf, *N.Jb. Geol. Paläont. Mh.*, 7 : 385 – 399.
- Anderson, G. 1975.** Coring and core analysis hand book., Pet. Publishing Company, Tulsa, 200 P.
- Boukhary, M. A. 1985.** Paleontological studies of the Eocene succession in western Qatar, Arabian Gulf, *Revue de Paléobiologie*. 4 : 253 – 273.

- Cavelier, C. 1970.** Geological description of the Qatar Peninsula, Dept. Petrol. Aff. Qatar : 1 – 39.
- Darcy, H. 1956.** Les fontaines publiques de la ville de Dijon. Dalmont, Paris, 674 pp.
- Davis, S. N. 1969.** Porosity and permeability of natural materials. Flow Through Porous Media, ed. R. J. M. De Wiest Academic Press, New York, : 54 – 89.
- El-Sayed, A. A. 1981.** Geological and petrophysical studies for the Algyó-2 reservoir evaluation, Algyó oil and gas field, Hungary., Ph. D. Thesis, Hungarian Academy of Sc., Budapest, 166 P, (unpublished).
- Giles, M. R. and J. D. Marshall 1986.** Constraints on the development of secondary porosity in the subsurface : re-evaluation of processes. Marine and Petroleum Geo. 3 : 243 – 255.
- Hamam, K. A. 1984.** Status of the stratigraphic nomenclature of Qatar. PED internal report, 20P.
- Hashimoto, H. and T. Saganuma 1973.** Field emission scanning microscope., JEOL News, c / o JEOL LTD, Tokyo – 196. 11 : 1 – 10.
- Hearn, C. L., W. J. Ebanks Jr., R. S. Tye, and V. Ranganathan 1984.** Geological factors influencing reservoir performance of the Hartzog Draw field, Wyoming. JPT. 36 : 1335 – 1344.
- Hutcheon, I. and A. Oldershaw 1985.** The effect of hydrothermal reactions on the petrophysical properties of carbonate rocks. Canadian Soc. of Petroleum Geo. 33 : 359 – 377.
- Levorsen, A. I. 1967.** Geology of petroleum (2nd ed.) Freeman, San Francisco, 724 P.
- Nicholas, K. C. and D. H. Krinsley 1971.** Comparison of stratigraphic and electron microscopic studies in Virginia Pleistocene coastal sediments. J. of Geo. 79 : 426 – 437.
- Purser, B. H. 1973.** The Persian Gulf, Berlin., Springer-Verlag: 179 – 191.
- Smith, K. C. A. 1961.** Scanning., p. 241 – 251, in Encyclopedia of microscopy. Reinhold, New York. 693 P.

بارامترات البنية لصخور الأيوسين الأسفل في قطر

عبد المقتدر عبد العزيز السيد

تم قياس بعض البارامترات البتروفيزيائية مثل المسامية والنفاذية والتوصيل الهيدروليكي لمينات صخرية جمعت من متكون الرس التابع للإيوسين الأسفل في قطر .

بمعالجة القياسات إحصائياً وصفت الصخور قيد الدراسة على أنها غير متجانسة الخصائص ، ولقد تم إستنباط علاقات تجريبية بين حجم الفراغات البينية وكل من المسامية والنفاذية والتي تميزت بمعاملات إرتباط عالية مما يتيح إمكانية إستخدامها في حساب كل من مقدرة الصخر على تخزين وتوصيل الموائع .

وباستخدام الميكروسكوب الألكتروني ودراسة الصور المجهرية للفراغات البينية تم تحديد الأسباب المحتملة لعدم تجانس كل من النفاذية والمسامية للصخور قيد الدراسة .